Published in final edited form as:

Atherosclerosis. 2016 June ; 249: 1–9. doi:10.1016/j.atherosclerosis.2016.03.032.

Biphasic alterations in coronary smooth muscle Ca^{2+} regulation in a repeat cross-sectional study of coronary artery disease severity in metabolic syndrome

Mikaela L. McKenney-Drake[1,2,*], **Stacey D. Rodenbeck**[1,*], **Meredith K. Owen**[1,3], **Kyle A. Schultz**[1], **Mouhamad Alloosh**[1], **Johnathan D. Tune**[1], and **Michael Sturek**[1]

[1]Department of Cellular & Integrative Physiology, Indiana University School of Medicine, 635 Barnhill Dr. Indianapolis IN, 46202

[2]College of Pharmacy & Health Sciences, Butler University, 4600 Sunset Ave. Indianapolis, IN 46208

[3]Covance, Inc. 671 South Meridian Road, Greenfield, IN 46140

Abstract

Background and Aims—Coronary artery disease (CAD) is progressive, classified by stages of severity. Alterations in Ca^{2+} regulation within coronary smooth muscle (CSM) cells in metabolic syndrome (MetS) have been observed, but there is a lack of data in relatively early (mild) and late (severe) stages of CAD. The current study examined alterations in CSM Ca^{2+} regulation at several time points during CAD progression.

Methods—MetS was induced by feeding an excess calorie atherogenic diet for 6, 9, or 12 months and compared to age-matched lean controls. CAD was measured with intravascular ultrasound (IVUS). Intracellular Ca^{2+} was assessed with fura-2.

Results—IVUS revealed that the extent of atherosclerotic CAD correlated with the duration on atherogenic diet. Fura-2 imaging of intracellular Ca^{2+} in CSM cells revealed heightened Ca^{2+} signaling at 9 months on diet, compared to 6 and 12 months, and to age-matched lean controls. Isolated coronary artery rings from swine fed for 9 months followed the same pattern, developing greater tension to depolarization, compared to 6 and 12 months (6 months= 1.8±0.6 g, 9 months= 5.0±1.0 g, 12 months= 0.7±0.1 g). CSM in severe atherosclerotic plaques showed dampened Ca^{2+} regulation and decreased proliferation compared to CSM from the wall.

Conclusions—These CSM Ca^{2+} regulation data from several time points in CAD progression and severity help to resolve the controversy regarding up- *vs.* down-regulation of CSM Ca^{2+}

Corresponding Author: Michael Sturek, Ph.D. 635 Barnhill Dr. Indianapolis, IN 46202; Phone: (317) 274-7772; Fax: (317) 274-3318; ; Email: msturek@iu.edu

*These authors contributed equally to this work

Conflict of interest

The authors declared that they do not have anything to disclose regarding conflict of interest with respect to this manuscript.

regulation in previous reports. These data are consistent with the hypothesis that alterations in sarcoplasmic reticulum Ca^{2+} contribute to progression of atherosclerotic CAD in MetS.

Keywords

Calcium regulation; smooth muscle phenotype; proliferation; Ossabaw swine

Introduction

Obesity affects more than one-third of adults in the United States[1]. The human propensity for obesity has been attributed to a "thrifty genotype"[2]. This "thrifty genotype" was adaptive during the early stages of human evolution, when humans were easily affected by the "feast or famine" environment associated with changing seasons and a lack of modern food preservation and storage. Now, a consistent and abundant food supply, coupled with a sedentary lifestyle, has propelled the obesity epidemic, resulting in the coining of such terms as "obesogenic environment"[3] and tongue-in-cheek references to a new species with the name "*Homo sedentarius*"[4]. Obesity often appears in connection with the metabolic syndrome (MetS), which is classically defined as the clustering of three or more of the following risk factors: central obesity, hypertension, dyslipidemia, insulin resistance, and glucose intolerance[5]. Together, obesity and MetS double the risk of coronary artery disease (CAD), the leading killer of Americans[6].

CAD is a progressive disease with stages typically classified according to the Stary classification system[7]. Early, clinically insignificant neointimal thickening due to lipid deposition in the artery wall worsens with increasing lipid and inflammatory cell infiltration[8, 9]. Further progression involves recruitment of coronary smooth muscle (CSM) cells from the media into the growing plaque. Such mobilization is accompanied by a shift in CSM phenotype from healthy, contractile CSM cells to synthetic, proliferative CSM cells[10], whose secretory capabilities result in the deposition of collagen and other fibers into the developing lesion. The presence of CSM cells in the atherosclerotic plaque stabilizes the early lesion. As atherosclerotic CAD progresses, however, increased apoptosis and accumulation of lipids and cellular debris within the plaque results in thinning of the fibrous cap surrounding the lesion. This thinning of the fibrous cap may lead to rupture and thrombosis, often resulting in myocardial infarction and sudden cardiac death.

Ca^{2+} is a ubiquitous second messenger known to be involved in smooth muscle contraction[10, 11], proliferation[10, 12–14], migration[15, 16], and gene transcription[17, 18]. Therefore, alteration in CSM Ca^{2+} regulation in CAD is an important area of study. Alterations in many Ca^{2+} transporters, including voltage-gated Ca^{2+} channels[19, 20], sarco-endoplasmic reticulum Ca^{2+} ATPases[19, 21, 22], transient receptor potential channels[23], plasma membrane Ca^{2+} ATPases[19], and Na^{+}/Ca^{2+} exchangers[19], have been described in CAD[24]. However, there is a paucity of data regarding time-dependent changes in CSM Ca^{2+} handling in the setting of obesity/MetS. This study utilized the well-characterized Ossabaw miniature swine model of MetS and CAD[22, 23, 25–28] to examine the changes in CSM Ca^{2+} regulation during obesity-induced CAD progression, providing a much needed longitudinal

assessment of Ca^{2+} regulation over time and with increasing severity. Further, we examined differences in Ca^{2+} regulation in CSM harvested specifically from plaque *vs.* vascular wall.

Materials and methods

Animal care and experimental groups

All experimental procedures involving animals were approved by the Institutional Animal Care and Use Committee at Indiana University School of Medicine with the recommendations outlined by the National Research Council and the American Veterinary Medical Association Panel on Euthanasia[29, 30]. Six month old Ossabaw miniature swine were fed 1 kg of an excess-calorie atherogenic diet daily for 6 (n=6), 9 (n=7), or 12 (n=9) months in the repeat cross-sectional study (Figs. 1 and 2). The 6 and 9 month time points were considered “early” and the 12 month time point “late” CAD for comparison to Lean healthy pigs. For comparison, an additional subset of Ossabaw miniature swine were fed the same excess-calorie atherogenic diet above for 11 months to provide coronary arteries for comparison of CSM in “mild CAD” and “severe CAD” defined as arteries with less than 30% and greater than 30% plaque burden, respectively, as assessed by IVUS (Fig. 3–5). Plaque *vs.* vascular wall components were dissected from the same artery segments in severe CAD to compare CSM properties (Fig. 4). Lean control swine for this dataset (n=6) were fed the standard diet mentioned above.

Metabolic phenotyping

Final body weights and blood were obtained at time of sacrifice for lipid analysis (ANTECH Diagnostics, Fishers, IN).

Intravascular ultrasound (IVUS) for quantification of coronary artery disease

Swine were anesthetized and intravascular ultrasound was performed as described previously[22, 23, 31, 32].

Still frame IVUS pullback images were obtained offline at 1 mm intervals (Fig. 1). Percent plaque burden measures were obtained using Image J software (1.48v, National Institutes of Health, USA).

Fluorescent imaging for assessment of CSM intracellular Ca^{2+} signaling from freshly harvested coronary arteries

CSM cells from Ossabaw swine were enzymatically isolated from freshly dissected coronary arteries and loaded with fura-2 AM (2.5 mmol/l Molecular Probes, Life Technologies, Eugene, OR) as previously described [19, 22, 23, 33].

Isometric tension studies for functional assessment of freshly harvested coronary arteries

Isometric tension was examined in isolated coronary artery rings (2–4 mm in length) as described previously[34].

Isolation of atherosclerotic plaques from coronary arteries with severe CAD

Following IVUS and sacrifice, coronary arteries were excised and cleaned of adherent tissue. Arteries were segmented and opened longitudinally. Artery segments with plaque burden greater than 30% as measured by IVUS were selected and labeled as “severe CAD” (n=5). Plaques such as those labeled as intima (I) in Fig. 4I “Severe CAD” histology were trimmed away from the artery wall and placed in conical tubes containing the same collagenase solution previously described for isolation of CSM cells from the coronary artery wall (media)[19, 22, 23, 33]. The plaque cell population was then isolated through a series of enzymatic washes. Plaque cells were loaded with fura-2/AM for 45 minutes, washed, and placed on ice prior to being imaged as described above.

Histology

Coronary artery segments (2–4 mm in length) were placed in 10% phosphate-buffered formalin for 24–48 hours, and then transferred to 70% ethanol. Histology was performed in the Department of Anatomy and Cell Biology at Indiana University School of Medicine (Indianapolis, IN).

Immunohistochemistry

Coronary artery segments embedded in paraffin (described above) were transported the Department of Pathology at Indiana University School of Medicine and were processed as previously described[32]. Immunostaining was performed using Ki-67 as a proliferation marker. Images were captured using a LEICA DM 300 inverted microscope and analyzed with ImageJ software.

Statistical analysis

Statistical analysis was performed using GraphPad Prism 5.0 (San Diego, CA). One-way analysis of variance (ANOVA) or two-way ANOVA with Bonferroni post hoc analysis was performed. Data are represented as mean±SEM. $p < 0.05$ was considered statistically significant.

RESULTS

Metabolic cCharacteristics

Swine fed an excess-calorie atherogenic diet developed MetS as indicated by increased body weight, hypertension, and elevated total cholesterol and triglycerides, (see Table 1 in associated Data in Brief article[35]). Plasma triglycerides and total cholesterol were decreased at 12 months of diet in the initial, repeat cross-sectional study. In contrast, total cholesterol was not different between mild and severe CAD groups in the 11-month diet study (data not shown).

Coronary artery disease (CAD) severity increases during prolonged MetS duration

Analysis of IVUS still-frames revealed increased coronary artery plaque burden MetS swine with time on atherogenic diet (Fig. 1D), but did not significantly increase until 12 months on diet. Percent wall coverage increased early in MetS-induced CAD, plateauing later (Fig. 1D;

solid line), indicating that atherosclerotic plaques expand around the circumference of the artery prior to encroachment upon the lumen. These data support our statement that percent wall coverage is a strong tool for quantification of early intimal CAD prior to the stage of more intimal plaque burden. These quantification methods suggest that swine on 6–9 months of atherogenic diet present with “early stage” CAD (representative IVUS still frame in Fig. 1B), whereas 12 months on atherogenic diet results in “late stage” CAD (representative still frame in Fig. 1C).

Coronary smooth muscle Ca^{2+} responses to depolarization are biphasically altered during disease progression

Fura-2/AM assessment of intracellular Ca^{2+} handling in response to depolarization revealed a biphasic pattern in CSM from swine with MetS, in which responses were heightened in “early state” CAD, followed by dampened responses in “late stage” CAD. Fig. 2A provides a representative tracing to demonstrate the experimental protocol. CSM from swine with “early stage” CAD after nine months of atherogenic feeding demonstrated greater Ca^{2+} influx through voltage-gated Ca^{2+} channels (VGCC) after activation by K^+ (80 mmol/L; Green shading; Fig. 2A) compared to cells from age-matched lean swine as quantified by area under the curve. This increased VGCC activation was absent in CSM from swine with “late stage” CAD (Fig. 2B).

Coronary artery responses to depolarization are biphasically altered during disease progression

Functional assessment of coronary rings from lean pigs revealed no effect of age on tension development to KCl (20 mM) (Fig. 2C; black bars). Rings from swine with MetS revealed a biphasic change in tension development to 20 mM KCl as CAD progressed (Fig. 2C; white bars). When compared to age-matched leans, rings from swine with “early stage” CAD after 9 months of atherogenic feeding developed significantly more tension to KCl (20 mM). Following 12 months of atherogenic diet feeding, tension development dramatically decreases below that of rings from lean age-matched swine (Fig. 2C).

Sarcoplasmic reticulum Ca^{2+} store capacity is altered during CAD progression

Release of the SR store with caffeine (5 mmol/L)-triggered activation of ryanodine receptors is observed as a transient, robust increase in cytosolic [Ca^{2+}] (blue arrow; Fig. 2A). This transient increase was significantly greater in CSM from swine with “early stage” CAD compared to CSM from age-matched lean swine. As observed with depolarization responses, this increased Ca^{2+} signal in CSM from swine with “early stage” CAD was absent in CSM from swine with “late stage” CAD (Fig. 2D).

Recovery of cytosolic [Ca^{2+}] following SR Ca^{2+} store release is biphasically altered during CAD progression

Finally, Ca^{2+} buffering impairment along with simultaneously store-operated Ca2+ influx was assessed after SR store depletion. This is observed as a sustained Ca^{2+} signal above baseline levels following SR Ca^{2+} store depletion with caffeine (red arrow; Fig. 2A). While

this revealed the same pattern of Ca^{2+} alterations during the time course of CAD progression, no significant changes from age-matched lean swine were observed (Fig. 2E).

Plaque burden and collagen content are increased with CAD severity

Arteries with greater than 30% plaque burden as assessed by IVUS were classified as having "severe" CAD, while arteries with less than 30% plaque burden were classified as having "mild" CAD. To further classify disease severity for more detailed analysis of plaque composition, histological analysis was performed. See lumen (L), intima (I), and media (M) layers labeled in Fig. 3A–C. Plaque burden in the "severe CAD" group was increased compared to that in the "mild CAD" group (Fig. 3G). An additional measure of intimal plaque growth is obtained when the intimal/medial area ratio (I/M) is assessed. I/M was significantly increased in severe CAD, compared to mild (Fig. 3H). Further, to assess progression of plaque fibrosis, collagen content within the plaque was examined and was increased ~30% in severe disease, compared to mild (Fig. 3I). Medial collagen content trended toward increase with severe CAD, but this was not significant (Fig. 3J; p=0.08).

Sarcoplasmic reticulum Ca^{2+} handling is altered with CAD severity

To examine steady-state SR [Ca^{2+}], the SR Ca^{2+} store was released with caffeine (5 mmol/l) in the absence of extracellular Ca^{2+} (See Fig. 4A for representative tracing/experimental protocol; "Caf-sensitive SR Ca^{2+} store"; bi-directional arrow) and the transient increase in cytosolic [Ca^{2+}] was measured. In CSM isolated from arterial segments with mild CAD a dramatic increase in caffeine-sensitive steady-state SR [Ca^{2+}] was observed (Fig. 4B). In contrast, CSM isolated from plaques of arteries with severe CAD showed depletion of the caffeine-sensitive steady-state SR [Ca^{2+}] compared to CSM isolated from both healthy and mild CAD swine. Following an increase in cytosolic [Ca^{2+}] resulting from caffeine stimulation, a number of extrusion/buffering mechanisms are employed to restore cytosolic [Ca^{2+}]. SERCA buffering activity is assessed by measuring the cytosolic [Ca^{2+}] undershoot below baseline levels during recovery from caffeine stimulation (see Fig. 4A; "SERCA Activity"; downward arrow). The cytosolic [Ca^{2+}] undershoot (SERCA activity) was increased in mild CAD and was dramatically decreased in CSM of arterial segments from severe CAD (Fig. 4C).

To provide an intra-arterial comparison, intracellular Ca^{2+} regulation in CSM harvested specifically from the intima (plaque) region was compared to CSM from the wall (media) of arteries with severe CAD. The caffeine-sensitive steady-state SR Ca^{2+} store was depleted in CSM from intima (plaque) compared to CSM from the artery wall (media) (Fig. 4D). Correspondingly, when CSM from the intima (plaque) was compared with the adjacent artery wall (media), plaque cells demonstrated a decreased undershoot, i.e. decreased SERCA activity (Fig. 4E).

L-type voltage-gated channel function is altered with CAD severity

To further and more specifically assess VGCC function, Ba^{2+}-containing depolarizing solution with low Na^{+} was employed. Ca^{2+} influx through VGCC immediately triggers activation of Ca^{2+} extrusion and buffering mechanisms, which makes direct assessment of VGCC activity difficult. Fura-2 binds Ba^{2+} with similar affinity as to Ca^{2+}. Substitution of

Ca^{2+} with Ba^{2+} allows Ba^{2+} entry through VGCC upon depolarization. Ba^{2+} is not buffered by SERCA or transported by the plasma membrane Ca^{2+} ATPase. Low extracellular Na^{+} inhibits Na^{+}/Ca^{2+} exchange, preventing Ba^{2+} extrusion by this pathway, thereby providing a pure measure of VGCC function. For a representative tracing and experimental protocol, see Fig. 4F.

The rate of Ba^{2+} entry was assessed as the slope of the rise in the F_{340}/F_{380} signal following depolarization. Rate of Ba^{2+} entry through VGCCs was dramatically increased in CSM from swine with mild CAD compared to Healthy and severe CAD (Fig. 4G). We also examined rate of Ba^{2+} entry following depolarization in the arterial wall (media) adjacent to the excised intima (plaque). VGCC activity was not different in CSM from plaques compared to CSM in their adjacent arterial media (Fig. 4H). The Healthy, Mild CAD, and Severe CAD histology with schematic illustrations of normal SR, increased SR, and decreased SR Ca^{2+} stores, respectively, are shown in Fig. 4I. The figure shows the proposed changes in Ca^{2+} handling associated with CSM phenotypic modulation during CAD progression.

Cell proliferation declines with CAD severity

To determine whether proliferation follows Ca^{2+} handling patterns, Ki-67 expression was measured as an index of proliferative activity within coronary artery sections (Fig. 5A–D). The number of proliferative cells within the intimal region of coronary arteries with severe CAD was dramatically reduced, compared to arteries with mild CAD (Fig 5E).

DISCUSSION

There is a paucity of literature on a time course analysis of the connection between MetS-induced CAD and CSM Ca^{2+} regulation. This study steps into the gap and provides insight into the transitory, biphasic nature of CSM Ca^{2+} regulation during the progression of CAD. Using *in vivo* intravascular ultrasound imaging we showed increased circumferential neointimal wall coverage in early CAD and more severe increased plaque burden in late CAD. The power of IVUS is that after the highly sensitive analysis of CAD progression the arteries are viable for interrogation of cellular Ca^{2+} signaling. We found increased Ca^{2+} influx and Ca^{2+} release and buffering by the sarcoplasmic reticulum in early CAD and a surprising reversal of these Ca^{2+} signaling events in more severe, late state CAD. By separating overt plaques away from medial CSM in the artery wall, we provide novel insight into heterogeneity of intracellular Ca^{2+} regulation in the different regions of severely diseased arteries.

This clarity is important because there has been confusion regarding differences in intracellular Ca^{2+} regulation observed in several studies of CAD. For instance, Witczak *et al.*[19] and Hill *et al.*[21] reported increases in SERCA expression and function. Witczak *et al.* and others[37] also demonstrated decreases in VGCC function with disease. However, Neeb *et al.*[22] demonstrated a decrease in SERCA function with disease, and several studies[20, 38, 39] reported an increase in VGCC function with disease. One possible explanation for the apparent discrepancy in the data is duration of diet and/or severity of disease. Indeed, diet duration is different in each of these studies, causing differences in disease severity. An additional factor in these discrepancies may be the swine model. Witczak[19] and Hill[21]

utilized diabetic dyslipidemic Yucatan swine that had no primary insulin resistance, while Berwick[20] utilized MetS Ossabaw swine with primary insulin resistance, hypertension, and increased aldosterone as major characteristics. Neeb[22] used both Ossabaw and Yucatan swine. Indeed, Neeb's work highlights model differences in SERCA function,[22] underscoring the need for time-dependent studies in the same model. Specific components of the Ossabaw swine model that may contribute to differences in Ca^{2+} regulation include primary insulin resistance and increased aldosterone[40]. The current study provides a repeat cross-sectional examination of intracellular Ca^{2+} regulation in MetS Ossabaw swine during CAD progression, reconciling the discrepant results in the reports mentioned above.

Here, we report that function of VGCC and SERCA is enhanced with early, mild CAD and that these functions decrease with increased CAD severity. These data explain, in part, the discrepancies in the reports mentioned above. During early, MetS-induced CAD, VGCC activity is increased, as observed by Berwick, *et al.*[20] At the same time, SERCA activity is increased, as observed by Witczak *et al*[19]. As MetS and CAD progress, however, VGCC and SERCA function are greatly diminished, which corresponds to the findings of Witczak[19] and Neeb[22]. This decrease in VGCC and SERCA function appears to occur concurrently with a reduction in cell proliferation, as measured by Ki-67 expression. Future studies will seek to determine whether these phenomena are causally linked.

Interestingly, in the repeat cross-sectional study, plasma triglycerides and total cholesterol were decreased after 12 months on atherogenic diet *vs.* 6 and 9 months, suggesting that plasma cholesterol could play a role in Ca^{2+} handling differences observed over CAD progression. This is unlikely, however, because the plasma cholesterol at 12 months was still increased ~4-fold above that of healthy lean pigs. Further, in the eleven month subset of swine used for analysis of Ca^{2+} handling in atherosclerotic plaque *vs.* media, total plasma cholesterol was not different in the mild *vs.* severe CAD groups, yet the decreases in SERCA and VGCC function persisted. These data suggest that the plasma cholesterol decrease in the repeat cross-sectional study did not explain the decrease in CSM Ca^{2+} handling in late CAD.

Additionally, this study provides new insight on intracellular Ca^{2+} regulation *within atherosclerotic plaque.* In the repeat cross-sectional study, CSM isolated from coronary arteries with "late" CAD were a mixed population of cells from the arterial wall and cells from the plaque. Here, for the first time isolating atherosclerotic plaques away from the artery wall, we provided a close-up look at CSM Ca^{2+} regulation within a plaque. Fig. 4D, E, and H provide strong evidence that SR Ca^{2+} handling is decreased in the intima (plaques) of arteries with severe CAD, compared to its adjacent wall (media). This finding prompts several questions: 1) Does a shift in Ca^{2+} regulation within atherosclerotic plaques signal a shift in the dominant cell phenotype within an atherosclerotic plaque? 2) If so, can intracellular Ca^{2+} handling provide insight regarding plaque stability and phenotypic modulation? These questions are beyond the scope of the current project, but are interesting areas of future investigation.

Together, the data in this report provide a much needed study of CAD progression in metabolic syndrome, providing insight on IVUS determinants of CAD severity and

histological analysis of cellular components of CAD progression. The study also highlights the need for additional studies to further solidify causal links between intracellular Ca^{2+} regulation, CSM proliferation, and alterations in atherosclerotic plaque morphology during CAD progression.

Acknowledgments

Financial support

This study was supported by National Institutes of Health (HL062552 and T32 DK064466), American Heart Association (15PRE25280001), Indiana CTSI Predoctoral TL1 Training Fellowship (TR000162), the Fortune-Fry Ultrasound Research Fund, and the Cardiometabolic Disease Research Foundation.

The authors wish to acknowledge James P. Byrd, Josh Sturek, and Brandy Sparks for wonderful technical support during the metabolic phenotyping phase of this study.

References

1. Ogden CL, Carroll MD, Kit BK, Flegal KM. Prevalence of childhood and adult obesity in the United States, 2011–2012. JAMA. 2014; 311:806–814. [PubMed: 24570244]
2. Neel JV. Diabetes mellitus: a “thrifty” genotype rendered detrimental by “progress”? Am J Hum Genet. 1962; 14:353–362. [PubMed: 13937884]
3. O’Rourke RW. Metabolic thrift and the genetic basis of human obesity. Ann Surg. 2014; 259:642–648. [PubMed: 24368636]
4. Levine JA. Lethal sitting: homo sedentarius seeks answers. Physiology (Bethesda). 2014; 29:300–301. [PubMed: 25180258]
5. Go AS, Mozaffarian D, Roger VL, Benjamin EJ, Berry JD, Blaha MJ, Dai S, Ford ES, Fox CS, Franco S, Fullerton HJ, Gillespie C, Hailpern SM, Heit JA, Howard VJ, Huffman MD, Judd SE, Kissela BM, Kittner SJ, Lackland DT, Lichtman JH, Lisabeth LD, Mackey RH, Magid DJ, Marcus GM, Marelli A, Matchar DB, McGuire DK, Mohler ER III, Moy CS, Mussolino ME, Neumar RW, Nichol G, Pandey DK, Paynter NP, Reeves MJ, Sorlie PD, Stein J, Towfighi A, Turan TN, Virani SS, Wong ND, Woo D, Turner MB. Heart disease and stroke statistics--2014 update: a report from the American Heart Association. Circulation. 2014; 129:e28–e292. [PubMed: 24352519]
6. Gami AS, Witt BJ, Howard DE, Erwin PJ, Gami LA, Somers VK, Montori VM. Metabolic syndrome and risk of incident cardiovascular events and death: a systematic review and meta-analysis of longitudinal studies. J Am Coll Cardiol. 2007; 49:403–414. [PubMed: 17258085]
7. Stary HC, Chandler AB, Dinsmore RE, Fuster V, Glagov S, Insull W Jr, Rosenfeld ME, Schwartz CJ, Wagner WD, Wissler RW. A definition of advanced types of atherosclerotic lesions and a histological classification of atherosclerosis. A report from the Committee on Vascular Lesions of the Council on Arteriosclerosis, American Heart Association. Circulation. 1995; 92:1355–1374. [PubMed: 7648691]
8. Libby P, Ridker PM, Hansson GK. Progress and challenges in translating the biology of atherosclerosis. Nature. 2011; 473:317–325. [PubMed: 21593864]
9. Rader DJ, Daugherty A. Translating molecular discoveries into new therapies for atherosclerosis. Nature. 2008; 451:904–913. [PubMed: 18288179]
10. Owens GK, Kumar MS, Wamhoff BR. Molecular regulation of vascular smooth muscle cell differentiation in development and disease. Physiol Rev. 2004; 84:767–801. [PubMed: 15269336]
11. Jiang H, Stephens NL. Calcium and smooth muscle contraction. Mol Cell Biochem. 1994; 135:1–9. [PubMed: 7816050]
12. House SJ, Potier M, Bisaillon J, Singer HA, Trebak M. The non-excitable smooth muscle: calcium signaling and phenotypic switching during vascular disease. Pflugers Arch. 2008; 456:769–785. [PubMed: 18365243]

13. Kruse HJ, Bauriedel G, Heimerl J, Hofling B, Weber PC. Role of L-type calcium channels on stimulated calcium influx and on proliferative activity of human coronary smooth muscle cells. J Cardiovasc Pharmacol. 1994; 24:328–335. [PubMed: 7526069]
14. Nilsson J, Sjolund M, Palmberg L, Von Euler AM, Jonzon B, Thyberg J. The calcium antagonist nifedipine inhibits arterial smooth muscle cell proliferation. Atherosclerosis. 1985; 58:109–122. [PubMed: 3004518]
15. Pauly RR, Bilato C, Sollott SJ, Monticone R, Kelly PT, Lakatta EG, Crow MT. Role of calcium/calmodulin-dependent protein kinase II in the regulation of vascular smooth muscle cell migration. Circulation. 1995; 91:1107–1115. [PubMed: 7850948]
16. Lundberg MS, Curto KA, Bilato C, Monticone RE, Crow MT. Regulation of vascular smooth muscle migration by mitogen-activated protein kinase and calcium/calmodulin-dependent protein kinase II signaling pathways. J Mol Cell Cardiol. 1998; 30:2377–2389. [PubMed: 9925373]
17. Hill-Eubanks DC, Werner ME, Heppner TJ, Nelson MT. Calcium signaling in smooth muscle. Cold Spring Harb Perspect Biol. 2011; 3:a004549. [PubMed: 21709182]
18. Wamhoff BR, Bowles DK, McDonald OG, Sinha S, Somlyo AP, Somlyo AV, Owens GK. L-type voltage-gated Ca2+ channels modulate expression of smooth muscle differentiation marker genes via a rho kinase/myocardin/SRF-dependent mechanism. Circ Res. 2004; 95:406–414. [PubMed: 15256479]
19. Witczak CA, Wamhoff BR, Sturek M. Exercise training prevents Ca^{2+} dysregulation in coronary smooth muscle from diabetic dyslipidemic Yucatan swine. J Appl Physiol. 2006; 101:752–762. [PubMed: 16763107]
20. Berwick Z, Dick G, O'Leary H, Bender S, Goodwill A, Moberly S, Owen M, Miller S, Obukhov A, Tune J. Contribution of electromechanical coupling between KV and CaV1.2 channels to coronary dysfunction in obesity. Basic Res Cardiol. 2013; 108:370. [PubMed: 23856709]
21. Hill BJF, Price EM, Dixon JL, Sturek M. Increased calcium buffering in coronary smooth muscle cells from diabetic dyslipidemic pigs. Atherosclerosis. 2003; 167:15–23. [PubMed: 12618264]
22. Neeb ZP, Edwards JM, Alloosh M, Long X, Mokelke EA, Sturek M. Metabolic syndrome and coronary artery disease in Ossabaw compared with Yucatan swine. Comp Med. 2010; 60:300–315. [PubMed: 20819380]
23. Edwards JM, Neeb ZP, Alloosh MA, Long X, Bratz IN, Peller CR, Byrd JP, Kumar S, Obukhov AG, Sturek M. Exercise training decreases store-operated Ca^{2+} entry associated with metabolic syndrome and coronary atherosclerosis. Cardiovasc Res. 2010; 85:631–640. [PubMed: 19744946]
24. Sturek M. Ca^{2+} regulatory mechanisms of exercise protection against coronary artery disease in metabolic syndrome and diabetes. J Appl Physiol. 2011; 111:573–586. [PubMed: 21596923]
25. Dyson MC, Alloosh M, Vuchetich JP, Mokelke EA, Sturek M. Components of metabolic syndrome and coronary artery disease in female Ossabaw swine fed excess atherogenic diet. Comp Med. 2006; 56:35–45. [PubMed: 16521858]
26. Lee L, Alloosh M, Saxena R, Van Alstine W, Watkins BA, Klaunig JE, Sturek M, Chalasani N. Nutritional model of steatohepatitis and metabolic syndrome in the Ossabaw miniature swine. Hepatology. 2009; 50:56–67. [PubMed: 19434740]
27. Wang HW, Langohr IM, Sturek M, Cheng JX. Imaging and quantitative analysis of atherosclerotic lesions by CARS-based multimodal nonlinear optical microscopy. Arterioscler Thromb Vasc Biol. 2009; 29:1342–1348. [PubMed: 19520975]
28. Sturek, M.; Tune, JD.; Alloosh, M. Ossabaw Island miniature swine: metabolic syndrome and cardiovascular assessment. In: Swindle, MM., editor. Swine in the Laboratory: Surgery, Anesthesia, Imaging, and Experimental Techniques. Boca Raton: CRC Press; 2015. p. 451-465.
29. Institute for Laboratory Animal Research. Guide for the care and use of laboratory animals. Washington, D.C: National Academy Press; 2010.
30. AVMA Panel on Euthanasia. American Veterinary Medical Association, 2000 Report of the AVMA panel on euthanasia. JAVMA. 2001; 218:669–696. [PubMed: 11280396]
31. Sturek, M.; Alloosh, M.; Wenzel, J.; Byrd, JP.; Edwards, JM.; Lloyd, PG.; Tune, JD.; March, KL.; Miller, MA.; Mokelke, EA.; Brisbin, IL, Jr. Ossabaw Island miniature swine: cardiometabolic syndrome assessment. In: Swindle, MM., editor. Swine in the Laboratory: Surgery, Anesthesia, Imaging, and Experimental Techniques. Boca Raton: CRC Press; 2007. p. 397-402.

32. McKenney ML, Schultz KA, Boyd JH, Byrd JP, Alloosh M, Teague SD, Arce-Esquivel AA, Fain JN, Laughlin MH, Sacks HS, Sturek M. Epicardial adipose excision slows the progression of porcine coronary atherosclerosis. J Cardiothorac Surg. 2014; 9:2–12. [PubMed: 24387639]
33. Heaps CL, Sturek M, Price EM, Laughlin MH, Parker JL. Sarcoplasmic reticulum Ca(2+) uptake is impaired in coronary smooth muscle distal to coronary occlusion. Am J Physiol Heart Circ Physiol. 2001; 281:H223–H231. [PubMed: 11406489]
34. Owen MK, Witzmann FA, McKenney ML, Lai X, Berwick ZC, Moberly SP, Alloosh M, Sturek M, Tune JD. Perivascular adipose tissue potentiates contraction of coronary vascular smooth muscle: influence of obesity. Circulation. 2013; 128:9–18. [PubMed: 23685742]
35. McKenney-Drake ML, Rodenbeck SD, Owen MK, Schultz KA, Alloosh M, Tune JD, Sturek M. Metabolic characteristics observed during a repeat cross sectional study of coronary artery disease progression in Ossabaw miniature swine. Data in Brief. 2015 Submitted.
36. Dineen SL, McKenney ML, Bell LN, Fullenkamp AM, Schultz KA, Alloosh M, Chalasani N, Sturek M. Metabolic Syndrome Abolishes Glucagon-Like Peptide 1 Receptor Agonist Stimulation of SERCA in Coronary Smooth Muscle. Diabetes. 2015; 64:3321–3327. [PubMed: 25845661]
37. Bowles DK, Heaps CL, Turk JR, Maddali KK, Price EM. Hypercholesterolemia inhibits L-type calcium current in coronary macro-, not microcirculation. J Appl Physiol. 2004; 96:2240–2248. [PubMed: 14752123]
38. Knudson JD, Dincer UD, Bratz IN, Sturek M, Dick GM, Tune JD. Mechanisms of coronary dysfunction in obesity and insulin resistance. Microcirculation. 2007; 14:317–338. [PubMed: 17613805]
39. Borbouse L, Dick GM, Asano S, Bender SB, Dincer UD, Payne GA, Neeb ZP, Bratz IN, Sturek M, Tune JD. Impaired function of coronary BK_{Ca} channels in metabolic syndrome. Am J Physiol Heart Circ Physiol. 2009; 297:H1629–H1637. [PubMed: 19749164]
40. Alloosh M, Pratt JH, Sturek M, Basile DP. Elevated renin and enhanced adrenal steroidogenesis in the Ossabaw miniature swine model of the metabolic syndrome (abstract). FASEB J. 2008; 22:736.737.

Highlights

- Atherosclerotic coronary artery disease (CAD) progresses around the circumference of the artery, followed by encroachment on the lumen.
- Sarco-endoplasmic reticulum ATPase (SERCA) activity is increased in early, mild CAD and decreased in late, severe CAD, and this is correlated with an increased sarcoplasmic reticulum Ca^{2+} store.
- Voltage-gated Ca^{2+} channel (VGCC) function is increased in early, mild CAD.
- Increased SERCA and VGCC function are associated with elevated proliferation in early, mild CAD.

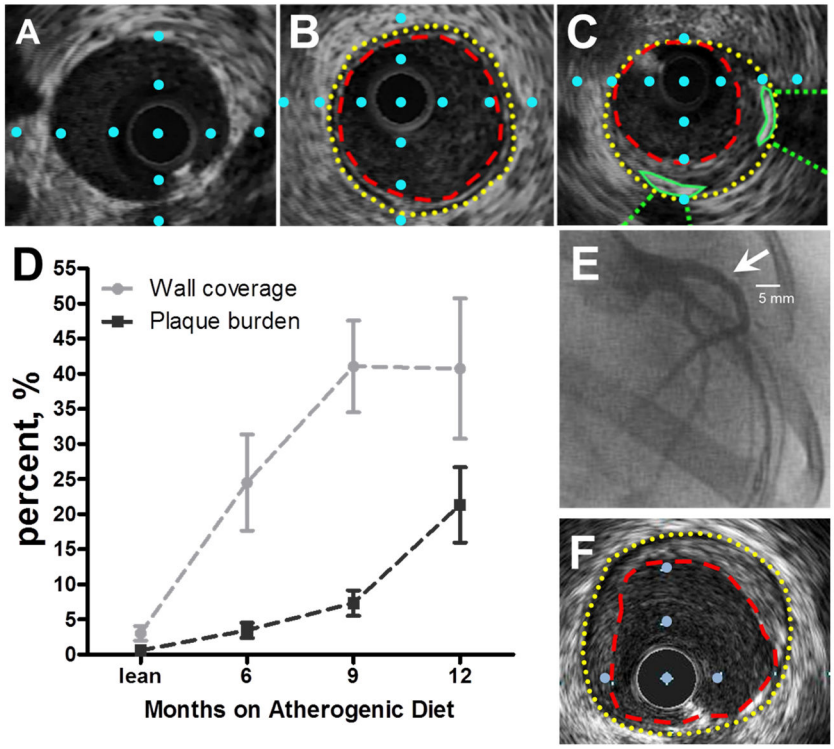

Fig. 1. Intravascular ultrasound imaging of coronary arteries with varying stages of coronary artery disease in the repeat cross-sectional study

(A) Cross-sectional view of a coronary artery from a lean pig. (B) Cross-sectional view of a coronary artery from a MetS pig with “early stage” CAD. Internal elastic lamina = yellow dotted line; lumen = red dashed line. (C) Cross-sectional view of a coronary artery from a MetS pig with “late stage” CAD. Distance between blue dots in A–C is 1 mm. (D) Wall coverage significantly increases in “early stage” CAD (0–9 months). Plaque burden does not increase until “late stage” CAD (>9 months). (lean= 4 pigs, MetS 6 months= 5 pigs, MetS 9 months= 5 pigs, MetS 12 months= 7 pigs). (E) Right anterior oblique coronary angiogram indicating lumen stenosis (arrow) in the left anterior descending artery. (F) IVUS still frame which corresponds to lumen stenosis in panel E.

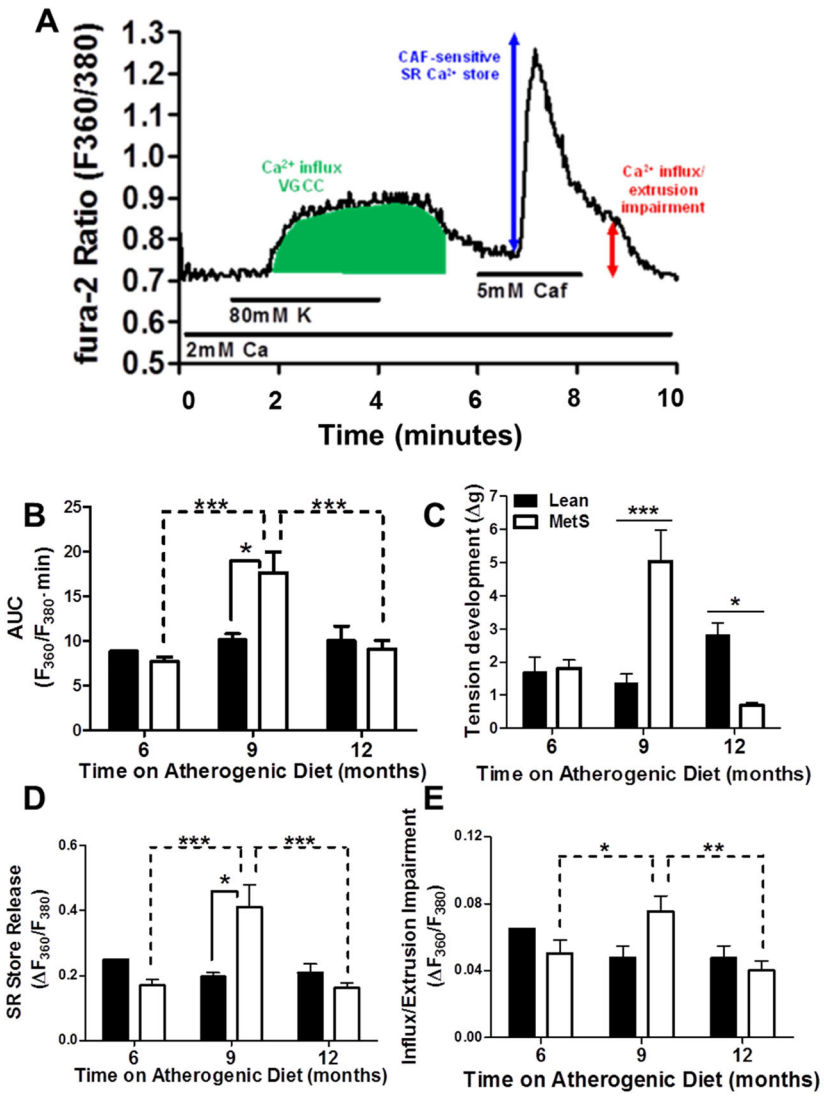

Fig. 2. Intracellular Ca^{2+} signaling is biphasically altered in coronary smooth muscle cells during CAD progression in the repeat cross-sectional study

(A) Representative tracing of CSM cytosolic Ca^{2+} flux. Labels indicate solution changes through superfusion chamber with duration shown by the horizontal lines. VGCC = voltage-gated Ca^{2+} channel; Caf = caffeine; green area under the curve = Ca^{2+} after 80 mM K+ membrane depolarization; blue double-headed arrow = SR Ca^{2+} store release; red double-headed arrow = delayed recovery to basal Ca^{2+} levels due to impaired Ca^{2+} buffering and store-operated influx. (B) 9 month duration of diet results in elevated Ca^{2+} influx following depolarization, compared to 6 and 12 months (dashed lines indicating significant differences) and to age-matched lean pigs (solid lines indicating significant differences). (C) Tension development to KCl (20 mM) in isolated coronary rings paralleled the changes in K depolarization-induced Ca^{2+} in panel B. (D) SR Ca^{2+} store release is elevated at 9 months on atherogenic diet, compared to 6 and 12 months (dashed lines indicating significant differences), and to age-matched lean pigs. € 9 months of atherogenic diet results in an increase in sustained Ca^{2+} signal, compared to 6 and 12 months, but not to age-matched

leans. (Lean = 9 pigs, cells = 60; MetS 6 months = 6 pigs, cells = 56; MetS 9 months = 7 pigs, cells = 68; MetS 12 months = 9 pigs, cells = 92)

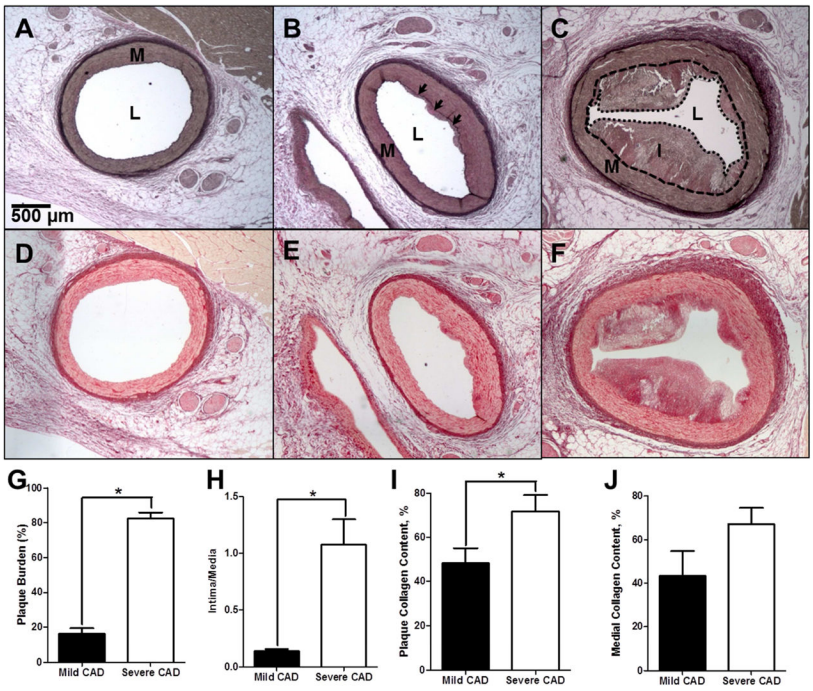

Fig. 3. Histological assessment of mild and severe CAD and collagen deposition

(A–C) Verhoeff-Van Giesen staining of elastin in a coronary arterial ring in lean (A), mild CAD (IVUS-detected plaque burden < 30%) (B), and severe CAD (IVUS-detected plaque burden > 30%) (C). L = Lumen; M = Media (Wall). I = Intima (plaque). Black arrows indicate the internal elastic lamina adjacent to early atherosclerotic lesion. (D – F) Picrosirius red staining of collagen deposition in lean (D), mild CAD (E), and severe CAD (F) coronary arterial rings. (G) % plaque burden is increased with severe CAD. (H) Intima/media ratio is increased with severe CAD. (I) Intimal collagen deposition is increased in severe CAD. (J) Medial collagen deposition demonstrates a trend (p=0.08) toward increase in severe CAD. (Mild CAD = 9 pigs; Severe CAD = 5 pigs)* p <0.05.

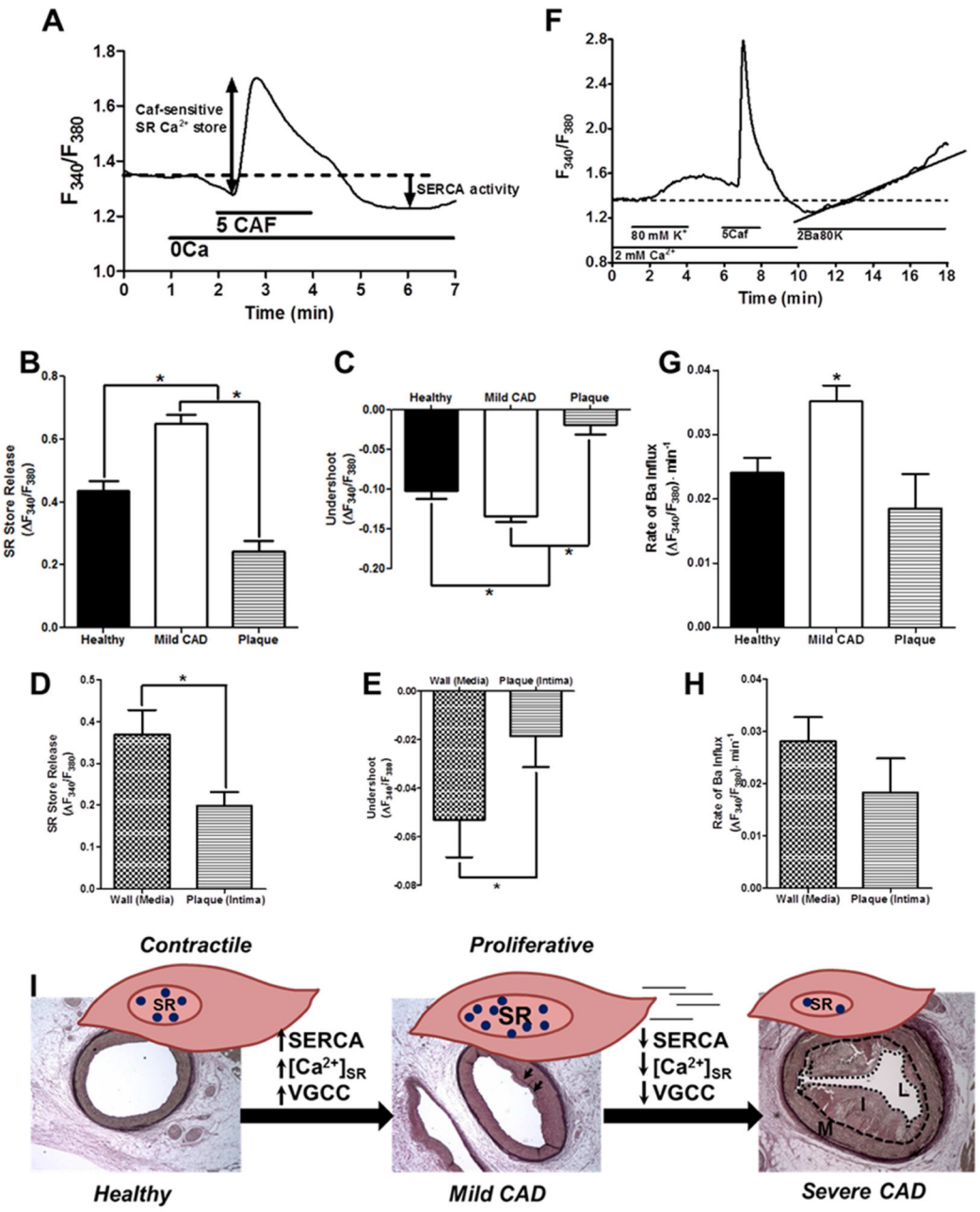

Fig. 4. Intracellular Ca^{2+} handling is biphasically altered with CAD severity

(A) Experimental protocol for panels B–E. (B) The caffeine-sensitive steady-state SR store is increased in mild CAD compared to both healthy lean and severe CAD. (C) The undershoot of cytosolic Ca^{2+} during recovery following removal of caffeine (SERCA activity) is increased in mild CAD compared to both healthy lean and severe CAD. (D) When compared with CSM isolated from the adjacent arterial media (wall), intimal (plaque) CSM display decreased caffeine-releasable steady-state SR Ca^{2+} store. (E) When compared with CSM isolated from the adjacent arterial media (wall), intimal (plaque) CSM display decreased SERCA activity. (Healthy = 6 pigs, cells = 67; Mild CAD = 9 pigs, cells = 156; Plaque = 5 pigs, cells = 29; Wall = 5 pigs, cells = 27). (F) Experimental protocol for panels

G–H. G. Rate of Ba^{2+} influx following depolarization is increased in CSM from mild CAD *vs.* Healthy and Severe CAD. (H) When compared to CSM from the media (wall) adjacent to the plaque, intimal (plaque) cells do not demonstrate a difference in Ba^{2+} influx. (Healthy = 6 pigs, cells = 72; Mild CAD = 9 pigs, cells = 151; Plaque = 5 pigs, cells = 25; Wall = 5 pigs, cells = 42). (I) Schematic depicting proposed changes in Ca^{2+} handling associated with CSM phenotypic modulation during CAD progression. Blue circles = Ca^{2+}.

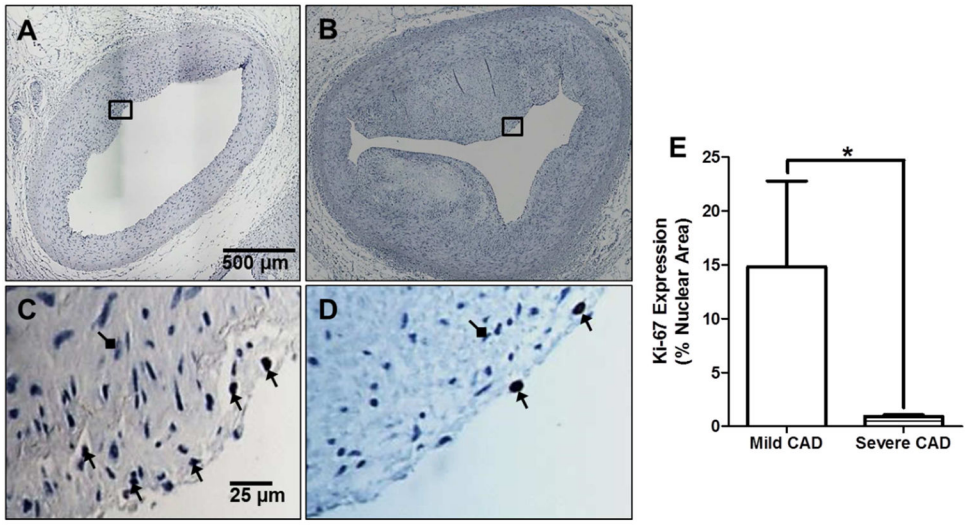

Fig. 5. Cellular proliferation is decreased in severe CAD

(A) Arterial ring from swine with mild CAD, interrogated with an antibody against Ki-67. (B) Arterial ring from swine with severe CAD, interrogated with an antibody against Ki-67. (C–D) Zoomed-in regions of rings in panels A and B. Black arrows indicate positive Ki-67 staining. Diamond arrows indicate negative Ki-67 stain. (E) Ki-67 expression is decreased in severe CAD. (Mild CAD = 8 pigs; Severe CAD = 5 pigs).